CONF-9006105--12

CONF-9006105--12

DE90 017831

THREE-DIMENSIONAL COMPUTER SIMULATION OF NON-REACTING JET-GAS FLOW MIXING IN AN MHD SECOND STAGE COMBUSTOR

S.L. Chang, S.A. Lottes and G.F. Berry
Argonne National Laboratory
9700 South Cass Avenue
Argonne, Illinois 60439

ABSTRACT

Argonne National Laboratory is investigating the non-reacting jet-gas mixing patterns in an MHD second stage combustor by using a three-dimensional single-phase hydrodynamics computer program. The computer simulation is intended to enhance the understanding of flow and mixing patterns in the combustor, which in turn may improve downstream MHD channel performance. The code is used to examine the three-dimensional effects of the side walls and the distributed jet flows on the non-reacting jet-gas mixing patterns. The code solves the conservation equations of mass, momentum, and energy, and a transport equation of a turbulence parameter and allows permeable surfaces to be specified for any computational cell.

The computer code treats the two different fluids (gas and jet) in the combustor by assigning two different temperatures for each flow and using local temperature to represent the mixture ratio. To allow jet penetration in a cross-stream direction, a jet entry model was developed. The entry model uses a one-cell nonpermeable channel next to each jet port to allow the jets to be with a specified velocity, controlled by the surface permeability of the entry channel. The simulation used a 41 by 21 by 13 grid system for the combustor. Four jet port arrangements including a 12-vertical-jet arrangement and three 8-vertical-4-horizontal arrangements (8 centered vertical jets, 8 side vertical jets, or 8 staggered vertical jets) were computed and compared. In general, the jets penetrate deep into the main flow and a large interface area is rapidly formed between jets and main flow promoting a high rate of convective mixing. Once the jets are turned into the downstream, mixing slows down dramatically as the steep gradients between jet and gas streams decay. Further mixing occurs primarily in turbulent and diffusive transport processes as the flow moves downstream. These gradient driven processes may be helped or hindered by the pattern of secondary flows established in the cross-stream through jet interaction as a consequence of jet port arrangement. Those arrangements which lead to the establishment of secondary flows or vortices in the Y-Z plane that sweep through the chamber corners appear to have the highest combined rates of thermal and momentum mixing. A computation of acceptable numerical convergence may need more than 1600 CPU seconds on a CRAY/XMP supercomputer.

NOMENCLATURE

A	Cross-sectional area in Y-Z plane (m^2)
D	Combustor width (m)
F	General function
k	Turbulent kinetic energy (J/kg)
H	Combustor height (m)
h	Enthalpy (J/kg)
L	Combustor length (m)
L_j	Jet port location in X-coordinate (m)
S	Source terms in conservation equations
T	Temperature (K)
U	Normalized axial velocity
u	Velocity (m/s)
X	Axial displacement coordinate (m)
Y	Vertical displacement coordinate (m)
Z	Horizontal displacement coordinate (m)

Greek Letters

β	Normalized temperature difference
ϕ	General dependent variable
Γ	Diffusion coefficient (turbulent and laminar)
ρ	Density (kg/m^3)
σ	Normalized cross-sectional deviation
τ	Average cross-sectional value

Subscripts

i,j	Summation index from 1 to 3
gas	Gas flow
jet	Jet flow

INTRODUCTION

Magnetohydrodynamics (MHD) power generation can attain higher overall efficiency and produce less air pollution than conventional coal-fired power plants [1]. The Department of Energy has been sponsoring the national coal-fired MHD development program including the development of a prototype 50 MWt coal-fired MHD combustor at TRW [2]. The coal-fired combustor (CFC) uses two-stage combustion processes to achieve design criteria: high electrical conductivity, high slag recovery, low heat loss, low unburned carbon carry-over, and stable combustion. In the first stage, pulverized coal is burned sub-stoichiometrically in a highly swirling preheated air stream to remove slag and maintain stable combustion. In the second stage, additional oxygen is injected to mix with the first stage combustion products and the mixture is burned to achieve a

---

high gas temperature. Tests have been performed to evaluate the effects of the non-uniformity of mixture temperature and velocity in the second stage combustor on the MHD channel performance. Poor jet penetration and jet-gas mixing are believed to be mainly responsible for the non-uniformity. Good mixing between the first stage sub-stoichiometric combustion products (or gas flow) and the oxidizer jets (or jet flow) would promote more uniform and complete combustion in the second stage [3,4].

Holdeman and Walker [5] and Rudinger [6] developed empirical models to predict penetration and mixing characteristics of jets in a confined crossflow based on experimental data and a self-similar flow principle. Scaling parameters like momentum flux ratio, mass ratio, and density were used to correlate the penetration and mixing parameters. In recent years, some numerical solutions of the deflected-jet situations have been reported. Patankar, Basu, and Alpay [7] used a comprehensive three-dimensional turbulent flow computer model and predicted the velocity field generated by a round jet deflected by a main stream normal to the jet axis with some success.

Experimental cold flow studies of the flow and mixing patterns in the second stage of a MHD coal-fired combustor have been conducted by TRW [8-10]. A one-third scale transparent model of the 50 MWt combustor was used. In order to determine the degree to which the secondary oxidizer mixes with the combustion products from the first stage, injector concentration measurements were taken throughout the flow cross-section at several axial stations downstream of the injector frame. To compare with the experimental measurements and enhance the understanding of combustor performance, Argonne National Laboratory (ANL) uses a three-dimensional hydrodynamics computer code and a two-dimensional combustion computer code to investigate the flow mixing and combustion processes in the MHD second stage combustor. The two-dimensional combustion code is used to simulate the two-fluid mixing and combustion processes and the three-dimensional code is used to study non-reacting jet penetration and jet-gas mixing patterns. At the present stage, ANL's investigation covers the non-reacting flow mixing simulations. This paper presents three-dimensional hydrodynamic results which compare the mixing patterns of four different 12-jet-port arrangements.

COMPUTATIONAL APPROACH

The COMMIX code developed at ANL [11] solves the conservation equations of mass, momentum, energy, and a transport equation of a turbulence parameter. The conservation equations possess a common form. If one denotes the general dependent variable ϕ to represent a scalar 1 in the continuity equation, three velocity components, u_i, i=1, 2, and 3, in momentum equations, enthalpy, h, in energy equation, and turbulent kinetic energy, k, in a one-parameter turbulence model, the conservation equations have the following form in a Cartesian coordinate system.

$$\partial(\rho u_j \phi)/\partial X_j = \partial(\Gamma_\phi \partial\phi/\partial X_i)/\partial X_i + S_\phi$$

The equations are solved by using a fully implicit algorithm in a staggered grid system. The details of the COMMIX code are described in reference 11.

Two different fluids (gas and jet) are mixed in the combustor. The COMMIX code can treat only one fluid in its solution procedure. Flows of two different temperatures are chosen to represent gas and jet flows. The COMMIX code computes enthalpy (or temperature) of a computational cell by averaging the enthalpies of both jet and gas flows in the cell on a mass basis. If the jet temperature is higher than the gas temperature, the mass fraction of the jet flow in a cell is primarily proportional to the temperature rise.

An important feature of COMMIX code is that it allows the users to specify permeable surfaces for a computational cell. To allow jet penetration in a cross-stream direction in a computer simulation, a jet entry model was developed. The jet entry model uses a one-cell non-permeable channel next to the injection port for each jet entry. The entry channel consists of four one-cell nonpermeable surfaces perpendicular to the jet flow direction and a partially permeable surface on the end of the channel. The jet entry model allows the jet to be injected into the cross-stream flow with a specified velocity, controlled by the surface permeability of the entry channel. The COMMIX code with this jet entry model was tested by comparing with a two-dimensional combustion computer code. The results showed good agreement.

Statistical parameters are used for comparing the degree of mixing between gas and jet flows under various conditions. For a Y-Z cross-section, the average of a general function F(Y,Z) is defined as,

$$\tau(X) = \iint F\, dA / A$$

and its normalized standard deviation is defined as,

$$\sigma(X) = [\iint (F-\tau)^2\, dA / A]^{1/2} / \tau$$

The general function F can be either temperature or axial velocity. The lower the temperature or velocity deviation the better the thermal or axial momentum mixing. If the flows are perfectly mixed, the average temperature is the bulk temperature and the temperature deviation becomes zero, and the velocity deviation drops to that of a fully developed turbulent channel flow.

JET PORT ARRANGEMENTS

Figure 1 shows an idealized CFC second stage combustor under investigation; it consists of four solid side walls (front, rear, top, and bottom), an inlet (left), and an exit (right). The first stage sub-stoichiometric coal combustion product (gas flow) enters the second stage combustor through the inlet to mix with additional oxidizer (jet flow) and complete the combustion. There are opposing jet ports on top, bottom, front, and rear walls. Jets on the top and bottom walls are referred to as vertical jets, while jets on the front and rear walls are referred to as horizontal jets. Four different 12-jet arrangements were investigated. One arrangement places 6 jets, evenly spaced, on each of the top and bottom walls (V1 to V6 of Figure 2). The other three arrangements have two jets on each of the front and rear walls at Y/D = 0.45 and 0.55 (H1 and H2 of Figure 2) and four jets on each of the top and bottom walls. The three arrangements with front and rear wall jet ports are called center, side, and staggered arrangements according to the position of jets on the top and bottom walls. These positions are derived by deleting pairs of opposing jets in the top and bottom walls (Figure 2). The center-jet arrangement deletes two pairs of jet ports V1 and V6, the side-jet arrangement deletes V3 and V4, and the stagger-jet arrangement deletes V2 and V5. Combustor geometry and simulation flow conditions are summarized in Table I.

Table I Combustor Geometry and Flow Conditions

Combustor Dimension (L:D:H) =	3.8:1:1
Jet Port Location (L_j/D) =	0.66
Pressure =	1 atm
Bulk Jet Concentration =	6.4 %
Jet Angle =	90 deg.
Jet Velocity =	614 m/s

The coordinate origin is set at the lower left corner of the inlet plane with X-, Y- and Z-axes in main flow (or axial), height (or vertical), and width (or horizontal) directions, as shown in Figure 1. A 41 by 21 by 13 grid system is defined for the computational domain of this geometry. For a symmetrical arrangement, only 41 by 11 by 7 nodes are used in the computation. Computation of a symmetrical case with good numerical convergence generally requires about 1600 seconds of CPU time on a CRAY/XMP supercomputer.

RESULTS AND DISCUSSION

The effects of the jet port arrangement on two types of mixing, thermal mixing and momentum mixing, are considered in analyzing the results. The development of mixing patterns is presented in Figures 3 through 14 in the form of contour plots of normalized temperature difference, contour plots of normalized X-direction (or axial) velocity, and plots of velocity vectors composed of the Y and Z components of velocity. The plots are shown at four X positions downstream of the jet injection position. Normalized temperature difference is defined as,

$$\beta = (T - T_{gas})/(T_\tau - T_{gas})$$

where T_{gas} is the inlet gas temperature and T_τ is the mean temperature. Normalized axial velocity is defined as,

$$U = u / u_\tau$$

in which u_τ is the average cross-sectional axial velocity (about 22 m/s).

The boundary conditions for all cases, inlet mass flow rates, velocities, temperatures, pressures, etc. are the same, except for the jet port arrangement on the walls at X/D = 0.66. Differences in the development of jet mixing in the downstream is therefore due to the variation of jet port arrangement.

The development of mixing for the case of 12 vertical jets is shown in Figures 3 to 5. The contours plotted in Figure 3 are for the normalized temperature difference, β. Contours of β = 1 represent the mean fluid temperature. The region of minimum value of β near the center of Figure 3a is the region the jets have not penetrated at X/D = 1.0. The impingement of jets in the center produces a set of sandwiched layers of hot and cold fluid in the downstream (Figures 3b and 3c). This layering provides a large interface area between hot and cold fluid, promoting thermal mixing. At downstream position X/D = 3.67, Figure 3d, the regions where layering occurred are fairly thoroughly mixed (fluid temperature is very near the mean).

Momentum mixing patterns for axial momentum in the case of 12 vertical jets can be seen in Figure 5. The jets, which are all located on the top and bottom walls in this case, constitute an obstacle to the main flow near the top and bottom walls at the injection position. The response of the main flow to these obstacles is in part to accelerate through the center of the channel as it interacts with the jets. This process creates a large region in the midrange of the Y-coordinate where the axial momentum is high and regions near the top and bottom walls where the axial momentum is low.

The velocity vectors for velocity components in the Y-Z plane, Figure 4a, show the even spacing of the opposed jets in the upstream. When the jets impinge, the relatively close, even spacing does not allow any significant degree of turning within the Y-Z plane, and therefore almost no secondary flow develops in the Y-Z plane as the main flow moves downstream (Figure 5c and 5d).

In the next three cases four of the vertical jets on the top and bottom walls are blocked, and the four horizontal jet positions on the front and rear walls (Figure 2) are opened. The impinging horizontal jets provide Z-momentum, which when interacting with the Y-momentum of the vertical jets may produce significant secondary flow patterns or vortices in the Y-Z plane as the flow develops downstream of the jets.

For the case with horizontal jets combined with centered vertical jets, thermal mixing proceeds rapidly in the region where the jets penetrate. The center and middle of the sides near the walls develops into a region with relatively well mixed warmer fluid, while the corners retain cooler fluid with steeper temperature gradients (Figure 6). Part of the reason for relatively poor mixing in the corners can be seen in the development of the secondary flow pattern in the Y-Z plane (Figure 7). With no jet momentum to sweep fluid out of the corners in the Y-Z plane, the secondary flow pattern develops with two vortices in each quadrant of the Y-Z plane, a very weak vortex near the corner and a relatively strong vortex between jet entry positions in the walls and the center of the chamber.

Both of the cases with horizontal jets combined with either staggered or side vertical jets exhibit the development of a secondary flow in the Y-Z plane with one vortex in each quadrant that sweeps fluid out of the corners into the chamber center region (Figures 10 and 13). This secondary flow process appears to aid both the thermal and axial momentum mixing. Figures 9, 11, 12, and 14 show the development of the mixing patterns downstream of the jets. In these cases by the last frame shown, at X/D = 3.67, a large portion of the central part of the chamber extending nearly to the walls and into the corners appears to be fairly well mixed.

A quantitative comparison of the degree of mixing for these jet arrangements can be made by the statistical measures of normalized deviation, σ, defined in the Computational Approach Section, of either temperature or axial velocity over a Y-Z plane.

Figure 15 shows a comparison of the normalized temperature deviation over a Y-Z plane versus position along the chamber length. All cases show a rapid drop in the cross section temperature deviation just downstream of the jet port position. This rapid mixing region extends only a short distance downstream where the jets are penetrating the main flow. Farther downstream, mixing proceeds primarily through the much slower gradient driven processes of turbulent or viscous diffusion, with some convective mixing still proceeding as a result of the development of secondary flows or vortices in the Y-Z plane. The three cases where jets were positioned near the corners all show a lower normalized temperature deviation over the exit plane than the case with centered jets.

Figure 16 shows the normalized velocity deviation over a Y-Z plane for the four jet arrangements. These results show that the axial velocity deviations for the arrangements which combine horizontal with vertical jets are all considerably lower than the arrangement that uses only vertical jets. By the exit plane the purely vertical jet arrangement has an axial velocity deviation over the exit plane that is much higher than the other arrangements.

While the measure of thermal mixing of the purely vertical jet arrangement is comparable to the arrangements of side and staggered vertical jets combined with centered horizontal jets, the measure of axial momentum unmixedness is much higher for the purely vertical jet arrangement.

CONCLUSION

A three-dimensional hydrodynamics computer code was used to investigate the flow mixing processes in an MHD second stage combustor. The flow and mixing patterns of four different jet port arrangements, including a 12 vertical jet arrangement and arrangements with 4 horizontal jets and either 8 centered vertical jets, 8 side vertical jets, or 8 staggered vertical jets, were computed and compared. Jet momentum is large enough so that the jets penetrate deeply into the main flow in all cases. The penetrating jets rapidly form a large interface area between jets and main flow promoting a high rate of mixing just downstream of the injectors. This initial high mixing rate may be viewed as convective mixing since it is driven primarily by expansion of the jets into the crossflow of the main stream. Once jet penetration has reached a maximum and the jets are turned into the downstream, mixing slows down dramatically as the steep gradients between jet and gas streams decay. Further mixing occurs primarily in turbulent and diffusive transport processes as the flow moves downstream. These gradient driven processes may be helped or hindered by the pattern of secondary flows established in the cross-stream through jet interaction as a consequence of jet port arrangement. Those arrangements which lead to the establishment of secondary flows or vortices in the Y-Z plane that sweep through the chamber corners appear to have the highest combined rates of thermal and momentum mixing.

ACKNOWLEDGEMENTS

This work is supported by U.S. Department of Energy, Assistant Secretary for Fossil Energy, under Contract W-31-109-ENG-38. Mr. Paul Lissac is appreciated for his assistance in preparing the figures.

REFERENCES

[1] "Open-Cycle Magnetohydrodynamic Electric Power generation, M. Petrick and B. Ya. Shumyatsky, eds., joint report of Angonne National Laboratory and U.S.S.R. Academy of Science (1978).

[2] Listvinsky, G., J. Alpay, L. Hil, K. King, D. Paul, D. Vanevenhoven, K. Natesan and D.Y. Wang "Development of a Prototypical MHD Coal Combustor," Proc. of 24th Intersociety Energy Conversion Engineering Conference, Washington, D.C., 2:965-970 (August 6-11, 1989).

[3] McClaine, A., J. Pinsley, and B. Pote, "Experimental Investigation on the Effects of the TRW Two-Stage Coal Combustor on the Performance of the AVCO Mk VI MHD Generator," Proc. of 24th Intersociety Energy Conversion Engineering Conference, Washington, D.C., 2:971-977 (August 6-11, 1989).

[4] Burkhart, T., G. Funk, R. Glovan, A. Hart, A. Herbst, J. Joyce, Y.M. Lee, S. Lundberg, and I. Stepan, "Coal-Fired MHD Topping Cycle Hardware and Test Progress at the Component Development and Integration Facility," Proc. of 23rd Intersociety Energy Conversion Engineering Conference, Denver, CO, 4:445-453, (July 31-August 5, 1988).

[5] Holdeman, J.D., and R.E. Walker, "Mixing of a Row of Jets with a Confined Crossflow," AIAA Journal, Vol. 15, No. 2, pp. 243-249, (1977).

[6] Rudinger, G., "Experimental Investigation of Gas Injection through a Transverse Slot into a Subsonic Cross Flow," AIAA Journal Vol. 12, No. 4, pp. 566-568 (1973).

[7] Patankar, S.V., D.K. Basu, and S.A. Alpay, "Prediction of the Three-Dimensional Velocity Field of a Deflected Turbulent Jet," Tran. of ASME, pp. 758-762 (Dec. 1977).

[8] Grove, A., et. al., "Cold Flow Modeling Study of Coal-Fired MHD Combustor," 26th Symposium on Engineering Aspects of Magnetohydrodynamics, Nashville, AL (1988).

[9] Grove, A., "Cold Flow Mixing Study of 50 MWt MHD Coal-Fired Combustor Second Stage," 27th Symposium on Engineering Aspects of Magnetohydrodynamics, Reno, NV (1989).

[10] Grove, A., et. al., "Cold Flow Mixing Study of an MHD Combustor Model Using Laser Velocimeter and Concentration Measurements," 28th Symposium on Engineering Aspects of Magnetohydrodynamics, Chicago, IL (1990).

[11] Domanus, H.M., R.C. Schmitt, W.T. Sha, and V.L. Shah, "COMMIX-1A: A Three-Dimensional Transient Single-Phase Computer Program for Thermal Hydraulic Analysis of Single and Multicomponents Systems," NUREG/CR-2896, ANL-82-25 (1983).

DISCLAIMER

Figures:

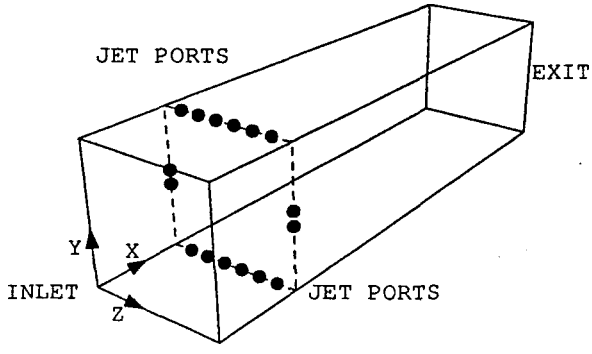

Figure 1 Idealized combustor geometry, MHD second stage

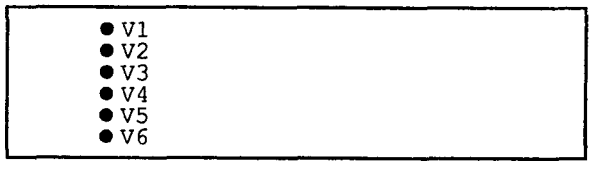

(a) Top or bottom wall

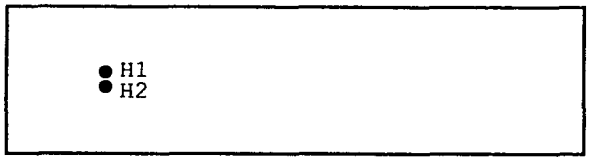

(b) Front or rear wall

Figure 2 Jet port locations

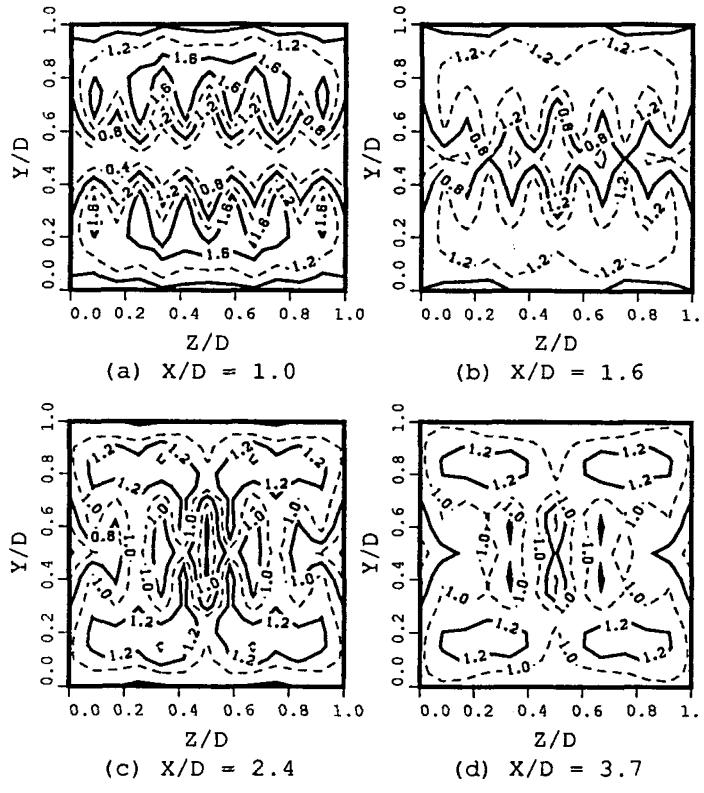

Figure 3 Development of thermal mixing (β contours, 12-vertical-jet)

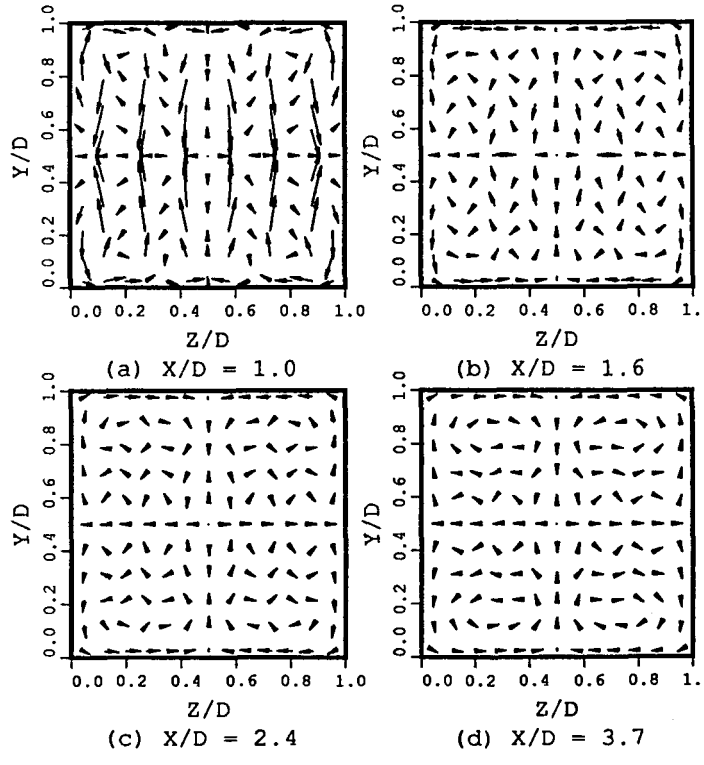

Figure 4 Development secondary flow (velocity vectors, 12-vertical-jet)

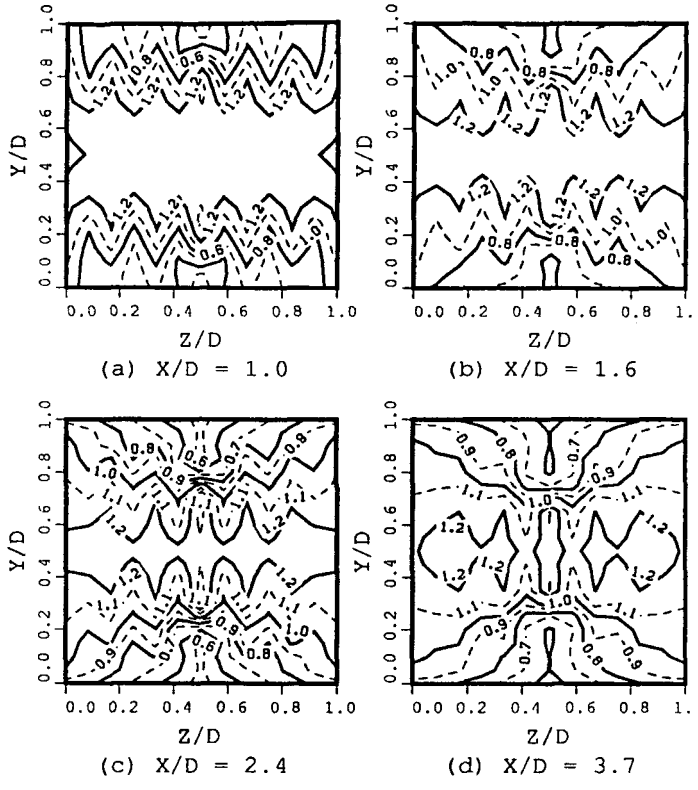

Figure 5 Development of momentum mixing
(U contours, 12-vertical-jet)

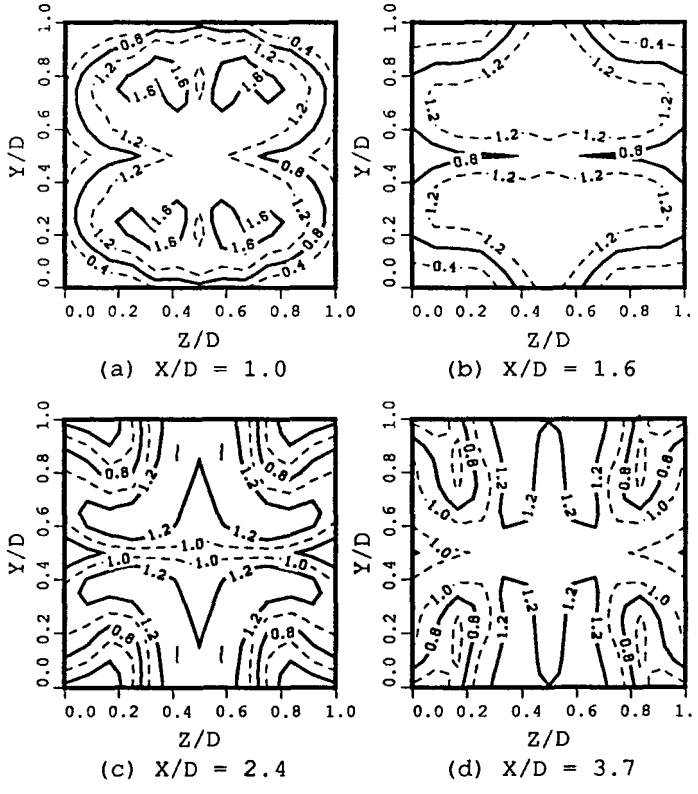

Figure 6 Development of thermal mixing
(β contours, center-8v4h-jet)

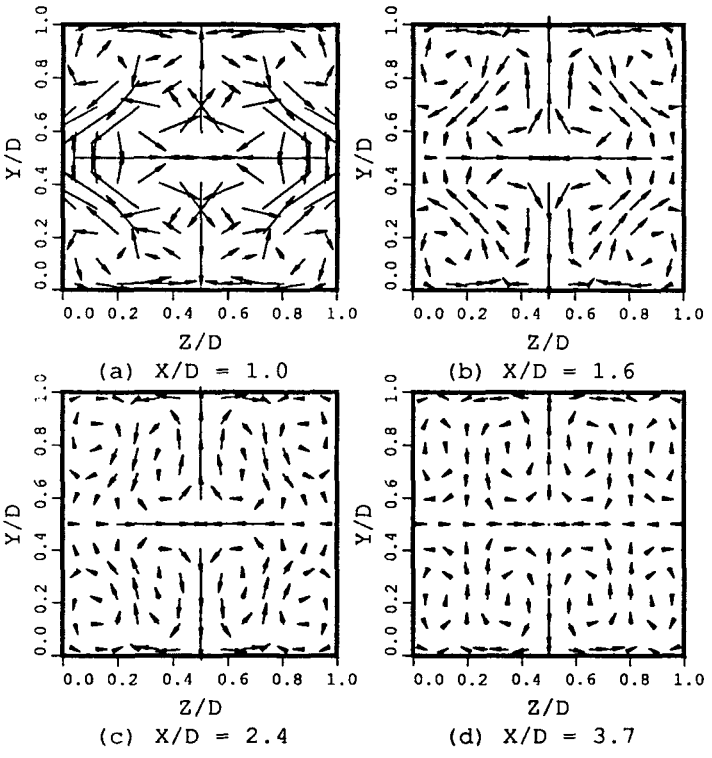

Figure 7 Development secondary flow
(velocity vectors, center-8v4h-jet)

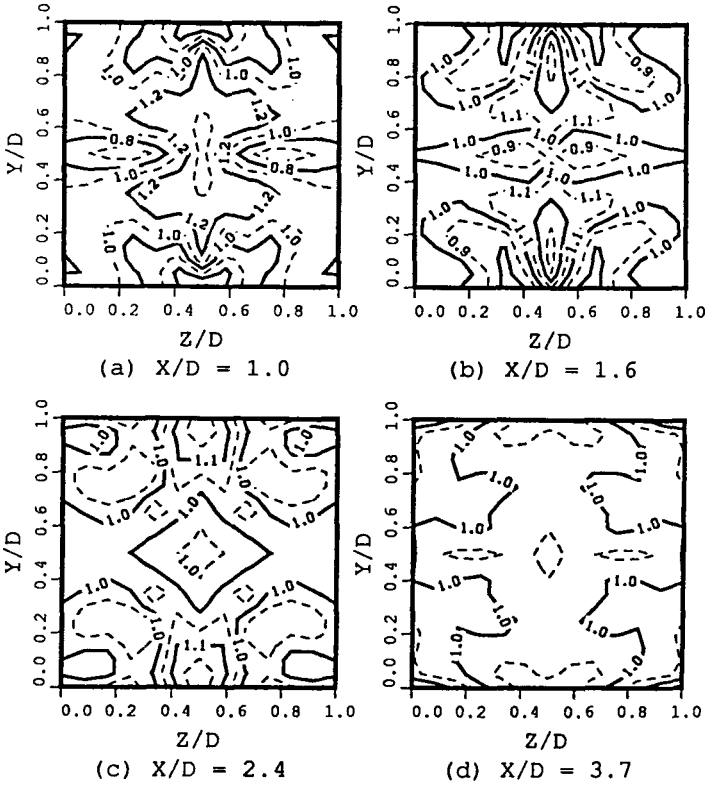

Figure 8 Development of momentum mixing
(U contours, center-8v4h-jet)

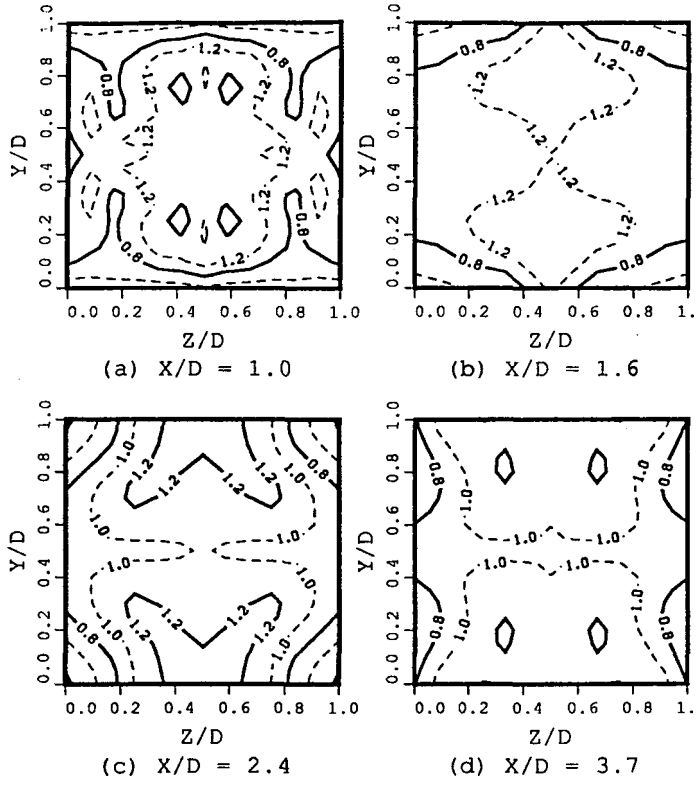

Figure 9 Development of thermal mixing
(β contours, staggered-8v4h-jet)

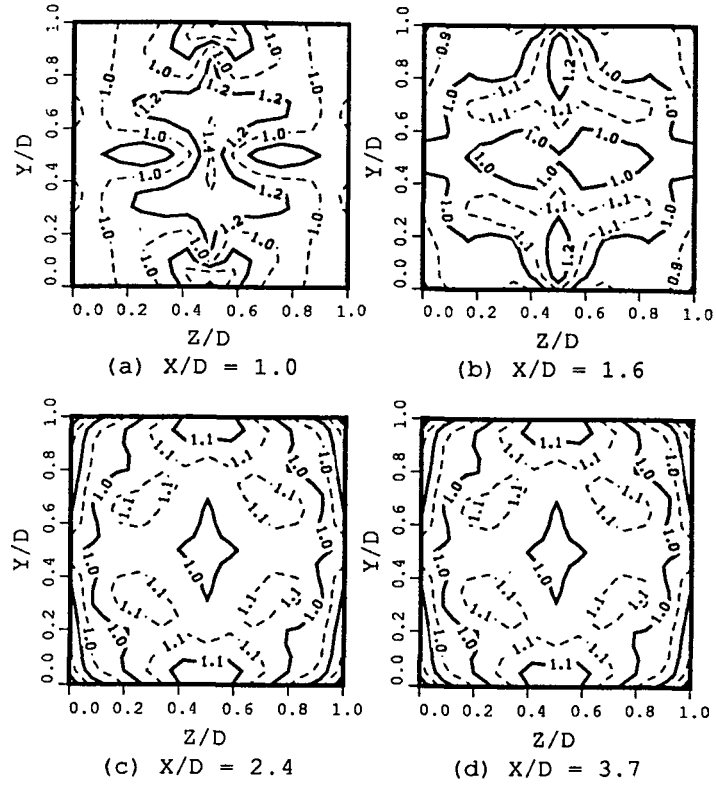

Figure 11 Development of momentum mixing
(U contours, staggered-8v4h-jet)

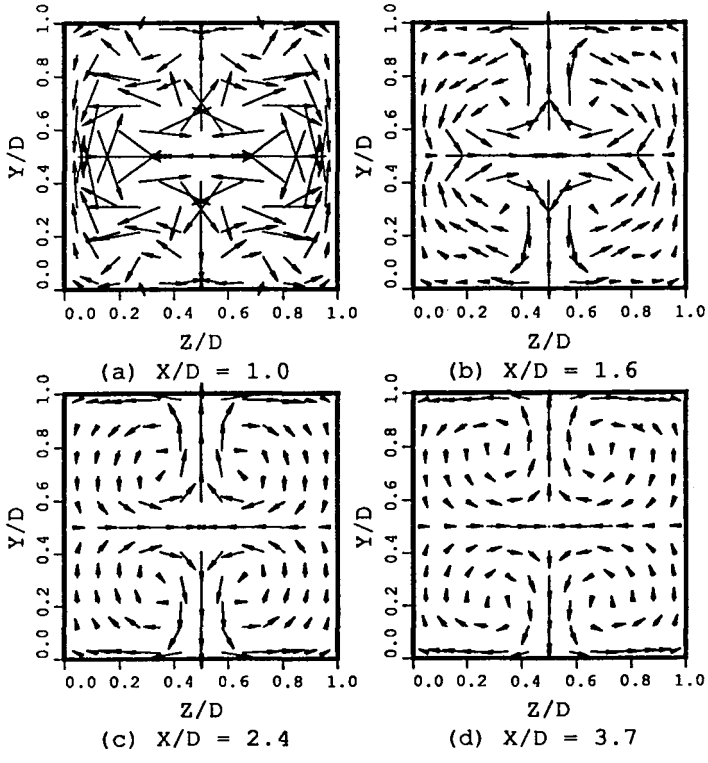

Figure 10 Development secondary flow
(velocity vectors, staggered-8v4h-jet)

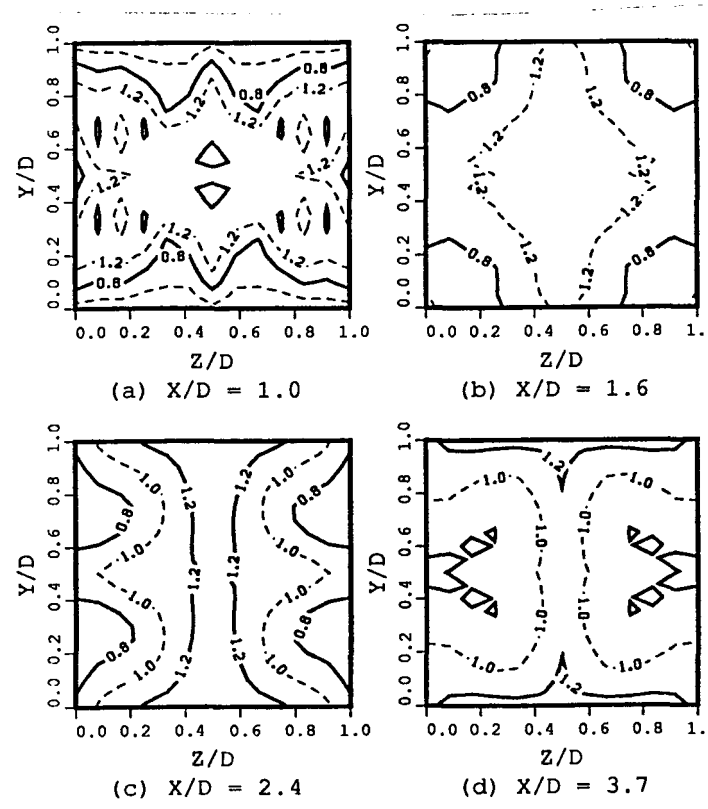

Figure 12 Development of thermal mixing
(β contours, side-8v4h-jet)

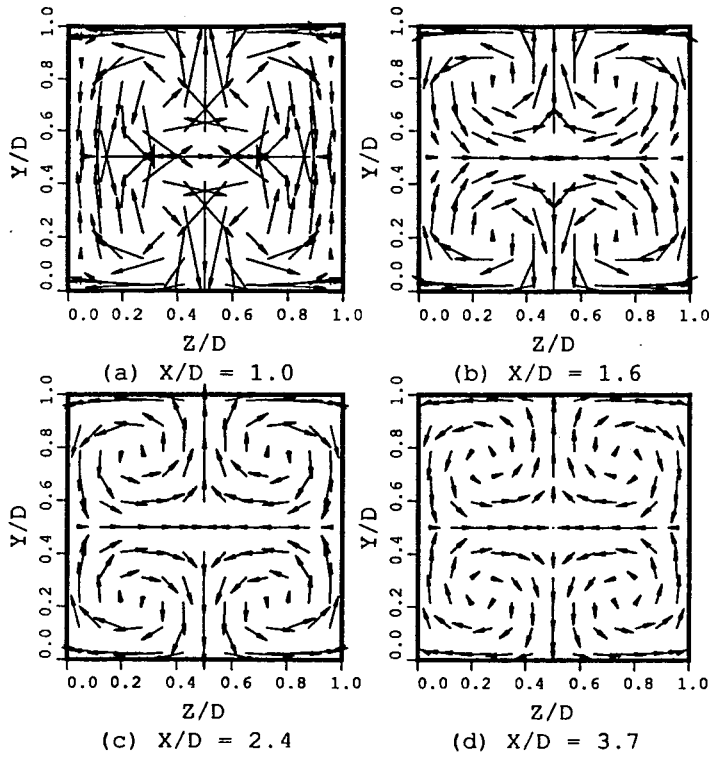

Figure 13 Development secondary flow
(velocity vectors, side-8v4h-jet)

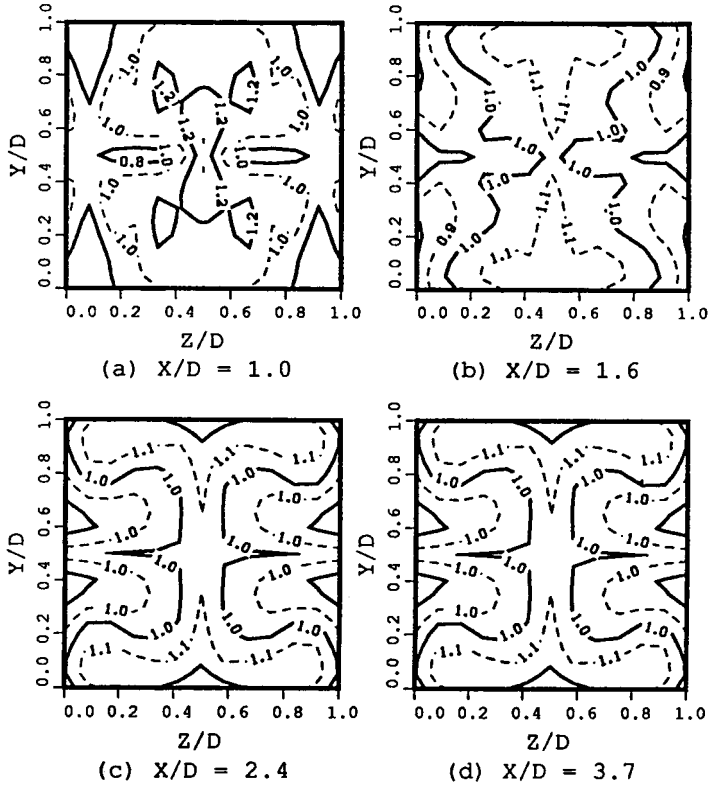

Figure 14 Development of momentum mixing
(U contours, side-8v4h-jet)

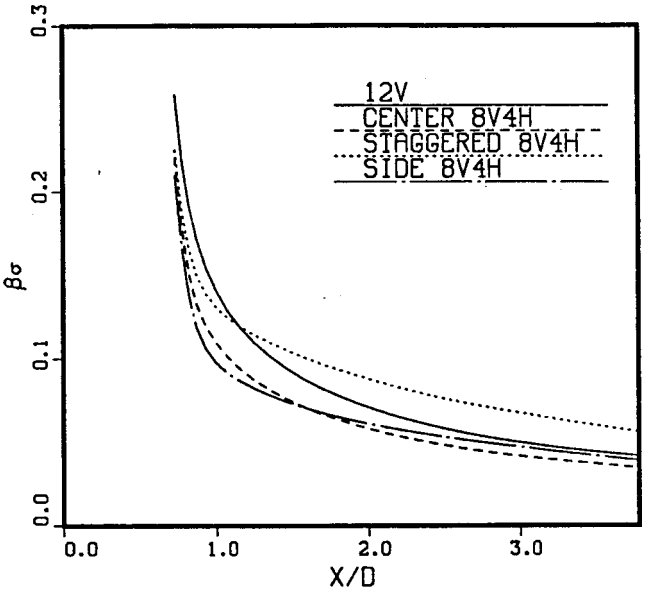

Figure 15 Comparison of temperature deviation

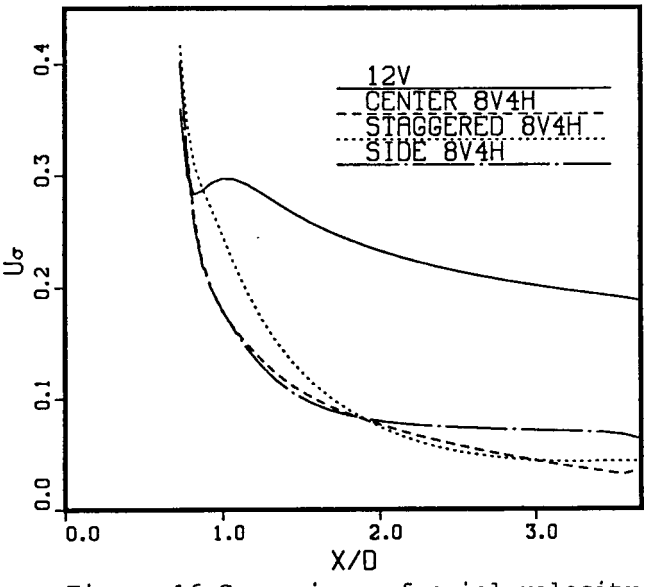

Figure 16 Comparison of axial velocity deviation